



# PET for *in vivo* pharmacokinetic and pharmacodynamic measurements

N. Gupta, P.M. Price, E.O. Aboagye\*

Cancer Research UK PET Oncology Group, Section of Cancer Therapeutics, Imperial College of Science, Technology and Medicine,  
MRC Cyclotron Unit, Hammersmith Hospital, Du Cane Road, London W12 ONN, UK

Received 19 September 2001; accepted 12 May 2002

## Abstract

Positron emission tomography (PET) scanning is evolving as a unique tool for drug development in oncology for improving both the efficacy of established treatment and in evaluating novel anticancer agents. As a non-invasive functional imaging modality, PET has an unrivalled sensitivity when monitoring the pharmacokinetics and pharmacodynamics of drugs and biochemicals when radiolabelled with short living positron-emitting radioisotopes. This is of particular relevance in assessing newer molecular-targeted therapy where conventional evaluation criteria (maximum tolerated dose and tumour shrinkage for example) may be inappropriate. PET has already been applied to a wide number of drugs to demonstrate activity *in vivo* from standard chemotherapy such as 5-fluorouracil (5-FU) [*J Clin Oncol* 17 (1999) 1580], to novel molecular agents such as those involved in tumour angiogenesis [*Br J Cancer* 83 (2000) P6] and antivasular therapy [*Proc Annu Meet Am Soc Clin Oncol* 19 (2000) 179a]. This review will evaluate the achievements of PET in the drug development process, an approach that promises to facilitate the rapid translation of scientific research into current clinical practice.

© 2002 Elsevier Science Ltd. All rights reserved.

**Keywords:** PET; Pharmacokinetics; Pharmacodynamics; Drug development; Novel anticancer drugs

## 1. Introduction

The field of oncology has undergone a revolution in drug discovery and therapeutic approaches led primarily through an increased understanding of genetic and molecular mechanisms in cancer evolution. Correspondingly, the previously held empirical random screening method in oncological drug development is being gradually replaced with the concept of rational drug design. This process identifies specific targets responsible for malignant cellular transformation and more importantly, drugs that can overcome them, rather than simply using the antiproliferative activity of a drug as an endpoint. New agents discovered for possible use as anticancer therapy include genes, proteins, growth factors and receptors, and those involved in specific pathways, for example, angiogenesis, signal transduction, cell cycle, cell apoptosis, invasion, meta-

stasis, drug resistance and blood flow. Further expansion of drug development has resulted from combinatorial chemistry, another new technology that has grown at a tremendous rate to produce a plethora of novel therapeutic targets [4]. However, drug development is still a protracted and expensive business. It is estimated that of 5000 possible drugs screened, only one drug is successfully approved and introduced into the market [5]. In addition, the candidate drug finally selected takes an average of 10 years of development and requires an investment of several million pounds before eventually proceeding to clinical trial [6]. Consequently, there is a need for an additional method of evaluating potential new drugs and to optimise existing treatment strategies. There is an increasing realisation that radio-tracer drug imaging as used in positron emission tomography (PET) has a major role to play in expediting drug development both in the clinical and preclinical setting, and which may in addition reduce the substantial costs currently incurred.

The objectives of drug development in oncology are clearly defined. The aims involve the determination of

\* Corresponding author. Tel.: +44-20-8383-3759; fax: +44-20-8383-2029.

E-mail address: eric.aboagye@ic.ac.uk (E.O. Aboagye).

optimum delivery of drug to the site of the tumour with minimum exposure to normal tissue, thereby achieving maximum therapeutic benefit. This requires accurate monitoring of drug pharmacology including pharmacokinetics (absorption, distribution, metabolism and elimination) and pharmacodynamics (tumour response, enzyme induction/inhibition receptor binding, tolerance, etc.). At present, these parameters are measured by analysis of blood and urine samples and occasionally using biopsy specimens of relevant tissues. Whilst this strategy is suitable for certain anticancer drugs, plasma monitoring may be irrelevant with the next generation of therapies such as anti-angiogenesis, where treatment is designed to target specific tissues. In this situation, the availability of a positron emitting radiotracer to quantify drug delivery and response in the relevant tissue can significantly advance our knowledge of drug pharmacology. The ability of PET to meet the challenges and demands of drug development relies on a multi-disciplinary team consisting of radiochemists, biologists, mathematical modellers, pharmacologists and clinicians.

## 2. Radiotracers

There are many positron emitting isotopes available for commonly occurring elements including carbon, oxygen, nitrogen and fluorine with half-lives ranging from seconds to several days (Table 1). They are usually made in a cyclotron, although some (copper 62) can be manufactured in a nuclear generator. Radiotracers are produced after replacement of a molecule in a compound of interest with a radionuclide without modifying their pharmaceutical, biological or biochemical properties. For example, positron emitting fluorine-18 is used as a substitute in fluorine-containing compounds, such

as in 5-fluorouracil (5-FU). In addition, fluorine-18 ( $^{18}\text{F}$ ) can be utilised instead of hydrogen in certain drugs, (as there is no suitable hydrogen isotope available), without compromising the behaviour of the molecule in the human body as with fluorinated anti-oestrogens [7].

An important consideration in PET is the half-life of the radionuclide. A radiotracer with a long half-life can be produced at a site different to that of actual administration, though multiple scans in one subject on the same day will not be possible. Alternatively, whilst radiotracers with a short half-life do permit sequential scanning on the same day, there are other limitations. Ideally, a radiopharmaceutical should be synthesised within 2–3 half-lives of the radionuclide to maintain high radiochemical yield and specific activity. This involves isolation of the target drug, purification, formulation into a sterile, pyrogen-free, isotonic solution and accurate quality control prior to injection. For drugs radiolabelled with carbon-11, which has a short half-life of 20 min, this necessitates manufacture at the site of delivery. Another disadvantage occurs if the drug to be studied has a long half-life (several hours) compared to the physical half-life of the label. Furthermore, as a result of the short physical half-life, larger amounts of radioactivity have to be handled. Generally, radiotracers with a very high specific activity (5000–15 000 mCi/mmol) are preferred so only small quantities ( $\mu\text{g}$ ) of stable compound are required. For these reasons, the potential exposure of staff involved with radiotracers remains high. To minimise this, rapid remote controlled and robotic-based chemistry has been designed and adopted for use by radiochemistry experts on site.<sup>8</sup>

At present, compounds containing *N*-, *S*-, or *O*-methyl (or -ethyl) groups, proteins and antibodies are fairly easily radiolabelled. It is not possible to radiolabel all drugs with sufficient radioactivity to derive useful information from them when used in investigational studies. This may occur if the length of synthesis and purification of the radiotracer is extensive and leads to substantial decay of radioactivity. Constraints in the availability of potential labelling reagents including precursors can also limit synthesis of radiotracers. The position of the radiolabel should be robust to avoid metabolic degradation, again restricting the number of compounds available. However, this can be fashioned advantageously when demonstrating the metabolic routes of specific compounds *in vivo*. It is anticipated that drug development authorities requiring PET imaging will begin to include precursor strategies into their drug development programmes to overcome these hurdles.

## 3. Acquisition and modelling of PET images

A 3D image of the distribution of the radiolabelled drug within the body comes from the simultaneous

Table 1  
A list of positron emitters and their half-lives

| Radioisotope   | Half-life | Positron decay (%) |
|----------------|-----------|--------------------|
| Bromine-75     | 98 min    | 76                 |
| Bromine-76     | 16.1 h    | 57                 |
| Carbon-11      | 20.4 min  | 99.8               |
| Cobalt-55      | 17.5 h    | 77                 |
| Copper-62      | 9.7 min   | 97.8               |
| Copper-64      | 12.7 h    | 19.3               |
| Fluorine-18    | 109.8 min | 96.9               |
| Gallium-68     | 68.1 min  | 90                 |
| Iodine-124     | 4.2 days  | 25                 |
| Iron-52        | 8.3 h     | 57                 |
| Nitrogen-13    | 10 min    | 100                |
| Oxygen-15      | 2.03 min  | 99.9               |
| Rubidium-82    | 1.25 min  | 96                 |
| Technetium-94m | 53 min    | 72                 |
| Yttrium-86     | 14.7 min  | 34                 |
| Zirconium-89   | 78.4 min  | 25                 |

detection of two gamma rays from the decay of the positron emitting radionuclide. The two 511 keV gamma rays are emitted at approximately  $180^\circ$  and are each recorded coincidentally by rings of external nuclear detectors, with the inference that the decay event occurred between the opposing two detectors. Data are obtained as sinograms that are reconstructed into tomographic images after correction for attenuation and detector efficiency. The data depict the spatial and temporal distribution of total radioactivity within a number of planes. Several physical restrictions impose a spatial resolution attainable with PET to 2–3 mm on clinical scanners (4–8 mm in most commercial scanners) and 0.5–1 mm on animal scanners. Images are analysed by defining a sample region or region of interest (ROI) on the PET scan after correlation with anatomical imaging and extracting radioactivity versus time curves from this area. This procedure is performed for several ROIs to allow analysis of tumour and normal tissue, for example liver and kidney.

Mathematical kinetic modelling of information derived from a PET scan expands data interpretation within a preconceived framework of important kinetic behaviour to obtain quantitative parameters of relevance. In practice, this involves comparing the concentrations of radioactivity in tissue (ROI) with that in arterial plasma and determining plasma-tissue exchange rate constants to construct a pharmacokinetic model.<sup>9</sup> Modelling is necessary for accurate calculation of all aspects of drug pharmacology, and to measure physiological variables such as tissue perfusion and metabolic rate. A tracer kinetic model is a mathematical description of the fate of the tracer in the human body, in particular the organ(s) under study. The usual method of establishing a mathematical description is to assign the possible distribution of tracer into a limited number of discrete compartments, within which tracer can be free, specifically or non-specifically bound. The compartments do not necessarily represent actual separate physical compartments, but are a simplification of complex biological interactions. A tracer kinetic model for [ $^{18}\text{F}$ ] fluorodeoxyglucose is illustrated in Fig. 1.

When drugs are not metabolised in the body, calculation of drug concentration is relatively straightforward. However, most drugs do undergo some metabolism *in*

*vivo* and metabolites are produced. This poses no difficulties if the metabolite does not contain the radio-tracer, but if it does, PET cannot distinguish the signal as coming from radiolabelled parent or radiolabelled metabolite. A number of strategies have been developed to extract the parent contribution from the total measured activity in this situation. One approach is correcting for metabolites by performing an additional scan of the radiolabelled metabolite. This has been applied for correction of 2-[ $^{11}\text{C}$ ] thymidine scans in which the principle metabolite is carbon dioxide, by doing a PET scan after administration of [ $^{11}\text{C}$ ]  $\text{CO}_2$  [10]. Alternative methods include, (1) mathematical modelling of metabolites, (2) washout strategies for radio-tracers with long half-life, where non-specific metabolites are allowed to be eliminated, leaving specifically bound species which are imaged at a late time point [11], or (3), by conducting paired studies, one of parent drug alone and one of parent drug combined with a compound to inhibit its metabolism [12].

Compartmental modelling relies on sufficient *a priori* knowledge of the tracers' outcome *in vivo* to construct a kinetic model. This can be problematic for anti-neoplastic agents due to tissue heterogeneity and often the lack of information on behaviour in the body. Special data-led approaches such as spectral analysis [13] and graphical analysis [14] have been explored as alternatives to compartmental modelling.

#### 4. PET and drug evaluation

There are a number of generic issues in drug development that can be addressed by PET imaging. These can be described in the form of questions: (1) does the drug sufficiently distribute to target (tumour) and how much goes to normal tissue, where toxicity may be produced, (2) how is the drug eliminated from tumour and normal tissue, (3) does the drug modulate its target in a predictable way, (4) is the drug efficacious. Points (1) and (2) can be classified as pharmacokinetic studies, and (3) and (4) can be broadly classified as pharmacodynamic studies. During this review, PET studies will be described under these two categories.

It is envisaged that for newer drugs there will be a change in paradigm, from ensuring that plasma concentrations which are associated with antitumour activity in rodents are achieved in humans, to ensuring that the degree of modulation of PET probes in rodent tumours (associated with activity) is achieved in humans.

##### 4.1. Pharmacokinetic studies

Despite extensive application in psychiatry and neurology in drug evaluation, PET has not yet reached its

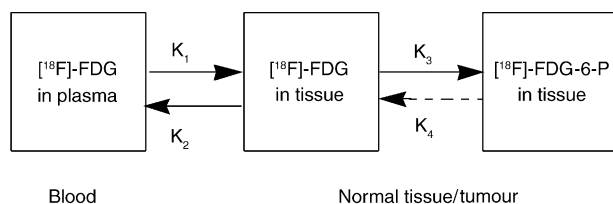


Fig. 1. Compartmental model of glucose utilisation for [ $^{18}\text{F}$ ]fluorodeoxyglucose.  $K_1$ ,  $K_2$ ,  $K_3$  and  $K_4$  are rate constants for delivery, washout, phosphorylation and dephosphorylation, respectively.

full potential in cancer therapeutics. PET can provide valuable information on drug pharmacokinetics in tumour and normal tissue by mathematical modelling of data. In some institutions, rapid plasma radioactive profiling during the PET scan can be used for calculation of plasma input function and to provide evidence of specific metabolic processes in humans and animals.

*In vivo* assessment of drugs can be performed following administration of radiotracer either alone (high specific activity) or mixed with cold (non-radioactive) drug (low specific activity). If the drug is of high activity, the total amount injected is minimal and the concentrations at these doses are much lower than the  $k_m$  for saturable metabolic processes. In this section, previous, ongoing and future work with PET will be reviewed.

#### 4.1.1. Temozolomide: evaluation of distribution and mechanism of action

Temozolomide is a new oral cytotoxic agent with good oral bioavailability, that has demonstrated anti-tumour activity against gliomas [15–18], malignant melanoma [19–21] and paediatric solid tumours [22,23]. No activity was seen against previously treated low grade non-Hodgkin's lymphoma (NHL) [24], hormone-refractory prostate cancer [25], untreated pancreatic adenocarcinoma [26], nasopharyngeal cancer [27] or soft-tissue sarcoma [28]. Temozolomide is an imidazotetrazine derivative, which though a prodrug, does not require metabolic activation to activate DNA alkylation, as does dacarbazine [29]. The drug undergoes pH-dependent ring opening and decarboxylation to 5-(3-methyl)-1-imidazole-4-carboxamide (MTIC) [30]. MTIC decomposes to 5-aminoimidazole-4-carboxamide (AIC) and methyl diazonium ion, which is assumed to be the reactive species that alkylates DNA (Fig. 2). Alkylation of DNA guanine in the O<sup>6</sup> position may be the primary cytotoxic event. PET studies using radiolabelled temozolomide have been performed to acquire knowledge about differences in tumour and normal tissue biodistribution and to confirm the proposed mechanism. It was anticipated that such data could help optimise therapy and patient selection.

Temozolomide was labelled with carbon-11 in either the 3-*N*-methyl or 4-carbonyl positions using a novel radiochemistry approach [31] (Fig. 3). Pharmacokinetics of [<sup>11</sup>C-*methyl*] temozolomide was investigated in conjunction with Phase 1 and 2 trials. Temozolomide exposure was greater in tumours compared with normal, contralateral brain (Fig. 4). Using spectral analysis [32], tumour uptake of temozolomide was found to be independent of tumour perfusion [33,34]. Tumour exposure to [<sup>11</sup>C-*methyl*] temozolomide derived radioactivity correlated with the duration of patient response, but not overall survival [35]. Continuing work involves the evaluation of the presumed mode of action of temozolomide. It was postulated that labelling temozolomide in the 3-*N*-

methyl position will result in incorporation of the radiolabel in DNA, whilst labelling in the 4-carbonyl position, will result in the loss of label as [<sup>11</sup>C] CO<sub>2</sub> in expired air prior to its incorporation into DNA (Fig. 3). Paired clinical studies have so far demonstrated higher levels of plasma and exhaled [<sup>11</sup>C] CO<sub>2</sub> for [<sup>11</sup>C-carbonyl] temozolomide compared with [<sup>11</sup>C-*methyl*] temozolomide [120].

#### 4.1.2. DACA: Pharmacokinetic assessment of DACA prior to conventional phase 1 trials

*N*-[2-(Dimethylamino)ethyl]acridine-4-carboxamide or DACA (XR5000) is a novel DNA-intercalating acridine derivative that stimulates DNA breakage via the formation of cleavable complexes between DNA and topoisomerase 1 and 2 [36]. It has a high activity against multi-drug resistant human tumour cell lines [37–39] and in experimental solid tumours such as implanted Lewis lung tumours in mice, with little ensuing myelosuppression [40]. This varied activity is thought to arise because DACA has dual interaction with both topoisomerases 1 and 2, and has ability to overcome P-glycoprotein and atypical (topoisomerase 2-mediated) multidrug resistance [37,38,40]. Other attractive properties exhibited by DACA such as high lipophilicity, suppression of ionisation of the acridine molecule at physiological pH, and capacity to cross the blood–brain barrier, led to the selection of DACA for clinical development. There were several important translational research questions that needed to be addressed including whether (1) the metabolic profile of DACA was altered in humans compared with pre-clinical models, (2) the drug distributed well to human tumours (predictive of activity), and (3) the degree of uptake into normal tissues was high, e.g. brain, (predictive of neurotoxicity). To address these issues, carbon-11 labelled DACA ([<sup>11</sup>C] DACA) was synthesised [41,42] and used in a pre-phase 1 radiotracer study to evaluate the tissue pharmacokinetics and plasma metabolite profile of DACA [43]. Prephase-1 studies were performed at a radiotracer dose equivalent to 1/1000 of the phase 1 starting dose (Fig. 5). To establish whether administration of pharmacological doses of DACA altered tracer kinetics, [<sup>11</sup>C] DACA tracer studies were repeated in patients undergoing phase 1 clinical trials [43,44]. Analysis of plasma samples in this pre-phase 1 and other studies show that DACA is extensively and rapidly metabolised [45–47]. Radioactivity was shown to localise in vertebra < brain < tumour < kidney < lung < myocardium < spleen < liver. The low peak concentrations and overall distribution of radioactivity in brain and vertebral bodies suggest that myelotoxicity and neurotoxicity are less likely to be dose-limiting. In contrast, high localisation of radioactivity was observed in the myocardium (which was saturable at phase 1 doses), implicating that cardiovascular toxicities may be dose-limiting. Tumour uptake of [<sup>11</sup>C] DACA was variable and demonstrated a moderate relationship with blood flow. This [<sup>11</sup>C] DACA work

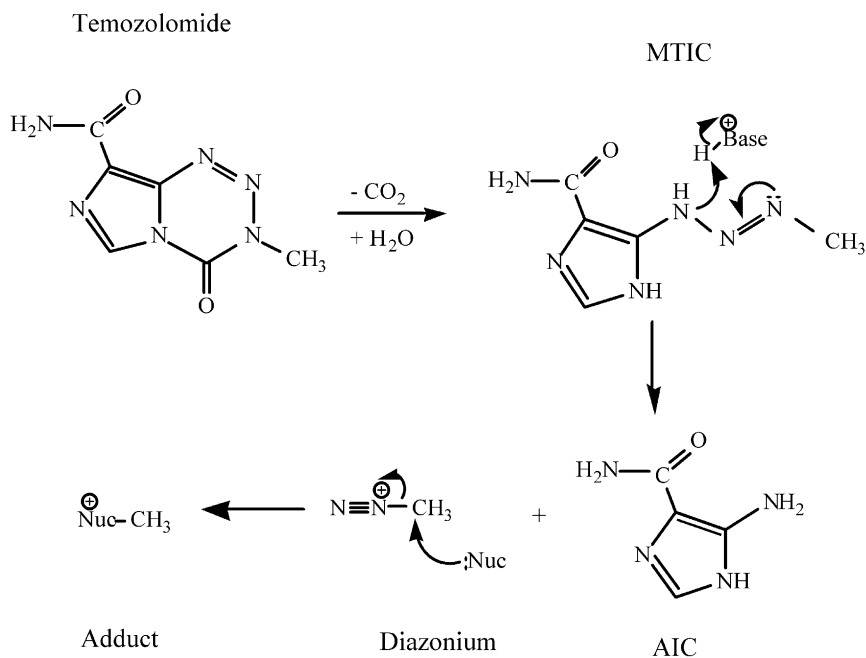


Fig. 2. Postulated mechanism of action of temozolomide.

constitutes the first such study using PET to provide information on intratumoral and normal tissue distribution data to aid drug development, and in particular, having the advantage of using such low levels of radiolabelled drug, so that toxicity would not be expected.

#### 4.1.3. 5-Fluorouracil: biomodulation of fluorouracil tissue pharmacokinetics

5-FU has been used either as a single agent or in combination chemotherapy regimes in many malig-

nancies including colorectal, gastrointestinal and breast cancers for over 30 years. As an antimetabolite, the action of 5-FU depends on its conversion to the anabolite 5-fluoro-2'-deoxyuridine-5'-monophosphate (FdUMP) via a series of enzymatic steps. FdUMP is responsible for inhibition of thymidylate synthase, which is necessary for the production of 2'-deoxythymidine-5'-monophosphate (TMP), a critical element in the repair and synthesis of DNA [48]. Up to 80% of systemically administered 5-FU is rapidly catabolised to an inactive toxic metabolite,  $\alpha$ -fluoro- $\beta$ -alanine (FBAL) by the

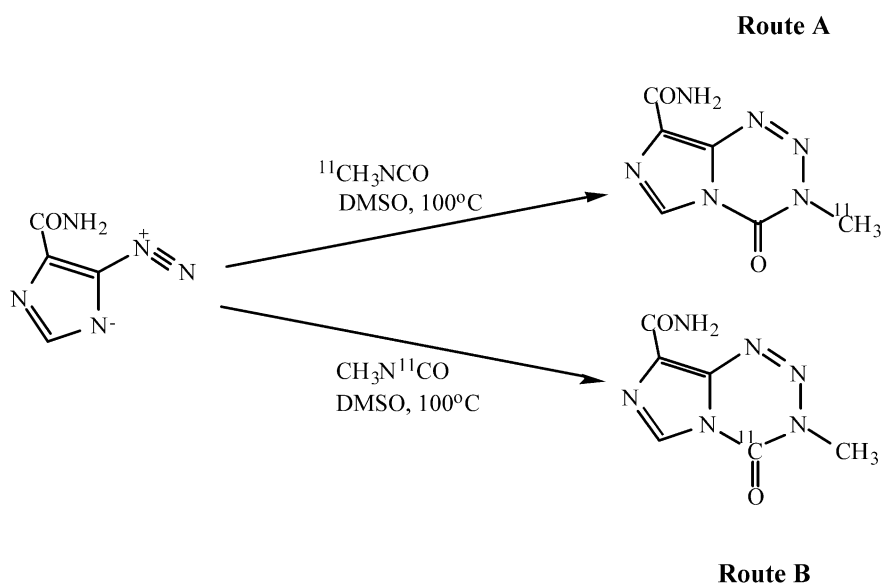


Fig. 3. Radiosynthesis of [ $^{11}\text{C}$ ]temozolomide in the 3-*N* methyl (Route A) or 4-carbonyl (Route B) position. The carbon in the 3-*N*-methyl position is assumed to remain with methyl diazonium which alkylates DNA, whilst that in the 4-carbonyl position is converted to carbon dioxide.

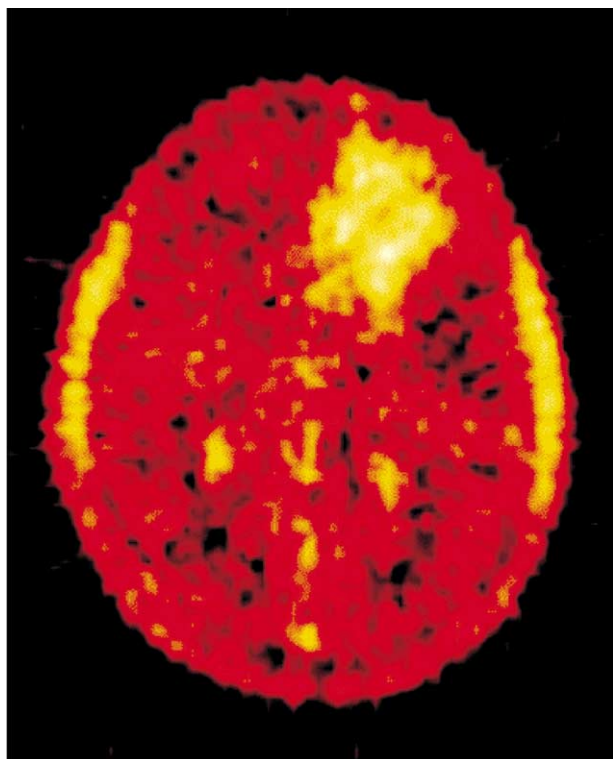


Fig. 4. Positron Emission Tomography (PET) [ $^{11}\text{C}$ -methyl]temozolomide image in a patient with glioma. Increased uptake is seen in the tumour compared with normal brain.

enzyme dihydropyrimidine dehydrogenase (DPD) [49]. Despite extensive experience and use of 5-FU, response rates and improvement in survival remains unsatisfactory. Different approaches have been developed to improve efficacy, such as biochemical modulation, dose and schedule modification, and regional drug-delivery systems.

The pharmacokinetics of 5-FU has been successfully investigated using radiotracers, and is the most common anti-cancer drug imaged with PET [51–55]. This is due to the ease of chemical synthesis of  $^{18}\text{F}$ -fluorouracil (5- $^{18}\text{F}$  FU) and the favourable half-life of fluorine allowing kinetic studies to be performed with good reproducibility [50]. Dynamic PET images for 5-FU in liver metastasis and normal tissue are illustrated in Fig. 6. From these and other results [56], it can be assumed that the high signal intensity in normal liver is an indication of its capacity to catabolise 5- $^{18}\text{F}$  FU to  $^{18}\text{F}$  FBAL. Furthermore, analysis of arterial blood by high performance liquid chromatography (HPLC) has detected the presence of 5- $^{18}\text{F}$  FU and high levels of  $^{18}\text{F}$  FBAL. This has been validated by magnetic resonance spectroscopy (MRS) studies which confirmed the presence of  $^{18}\text{F}$  FBAL [56]. The increase seen in kidney activity with time is consistent with elimination of 5-FU and associated metabolites. A pharmacodynamic rela-

tionship between tumour uptake of 5-FU and response, first seen in mice [57] has also been demonstrated in humans by PET methodology [58,59]. Studies showed that colorectal liver metastases with a higher uptake of 5-FU at 2 h, as measured by a standard uptake value (SUV) had a negative growth rate, whereas those with a low SUV had disease progression. These results have also been obtained using MRS studies of 5- $^{18}\text{F}$  FU [60,61].

PET has helped examine whether different compounds can biomodulate 5-FU pharmacology to increase the therapeutic ratio and antitumour activity. One study [1] examined the differences in pharmacokinetics of 5- $^{18}\text{F}$  FU in combination with folinic acid, alpha interferon ( $\text{IFN}\alpha$ ) or *N*-Phosphacetyl-L-aspartate (PALA), in addition to clinical trials that have previously shown variable benefit in patients with colorectal cancer. Results demonstrated that blood flow to the tumour was an important determinant of tumour exposure to total  $^{18}\text{F}$  radioactivity (consisting of fluorine-18 radiolabelled 5-FU, anabolites and catabolites). The relevance of drug delivery in the initial uptake and retention of radioactivity was emphasised by a significant correlation between tumour blood flow and tissue exposure to  $^{18}\text{F}$  radioactivity at 8 and 60 min. Blood flow to the tumour, and hence tumour exposure to 5- $^{18}\text{F}$  FU showed significantly reduced radioactivity after modulation with PALA and a non-significant increase was seen with  $\text{IFN}\alpha$ . However, no changes in tumour pharmacokinetics were seen with 5-FU when given in conjunction with folinic acid.

Another strategy to enhance the systemic activity of 5-FU has concentrated on inhibition of dihydropyrimidine dehydrogenase, which is the proximal and rate-limiting catabolic enzyme responsible for the degradation of 5-FU. Eniluracil is an oral DPD inhibitor [62] and its affect on the metabolism of 5-FU has been studied using PET. As high radioactivity is observed in normal liver after 5- $^{18}\text{F}$  FU due to accumulation of radiolabelled parent and metabolite, proof of principle of action of eniluracil was formulated to show a decrease in radiotracer uptake and retention of 5- $^{18}\text{F}$  FU in normal liver. This study demonstrated that in eniluracil-naïve patients, 5- $^{18}\text{F}$  FU derived radioactivity localised more strongly (0.0234% of the injected activity per ml at 11 minutes) in normal liver than in liver metastases (0.0032%) [12]. There was a distinct localisation of radioactivity in the gallbladder consistent with hepatobiliary clearance of  $^{18}\text{F}$  FBAL-bile acid conjugates. By contrast, after eniluracil administration, a substantial reduction of radiotracer exposure in normal liver and kidneys was seen, with no uptake in the gallbladder (Fig. 7). Another effect observed was an increase in plasma uracil and unmetabolised 5- $^{18}\text{F}$  FU levels and prolongation of radiotracer half-life from 2.3 to >4 h with eniluracil. This study illustrates how PET



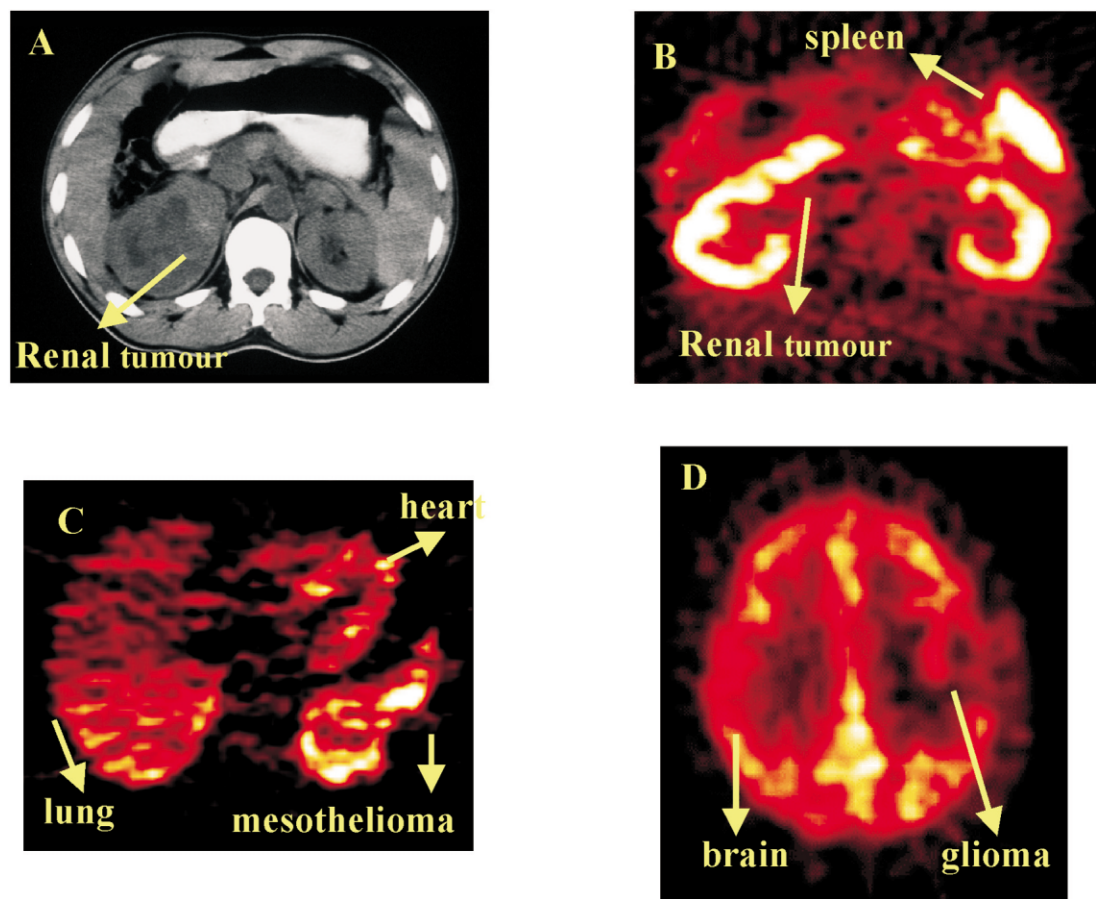


Fig. 5. Transaxial abdominal Computed Tomography (CT) scan (top left) and corresponding Positron Emission Tomography (PET)-[<sup>11</sup>C]N-[2-(dimethylamino)-ethyl]acridine-4-carboxamide] (DACA) image (top right) demonstrating radiotracer uptake in kidneys, spleen and renal tumour. Uptake of radiotracer is seen in heart, and mesothelioma (bottom left) and brain and glioma (bottom right). Reproduced with permission from Lippincott Williams & Wilkins (*J Clin Oncol* 2001, **19**(5), 1424, Fig. 2)

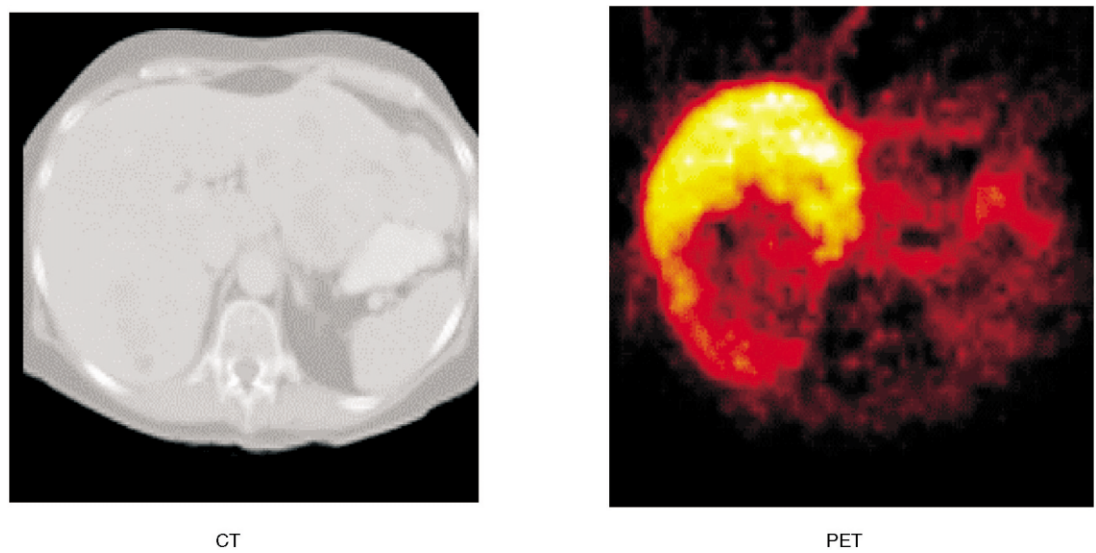


Fig. 6. Transaxial Computed Tomography (CT) (Left) and PET image after injection of 5-[<sup>18</sup>F]FU (right) of the abdomen of a patient with meta-static colorectal carcinoma. Images show liver with metastasis in left lobe, with corresponding large photopenic area seen on PET scan.

can provide *in vivo* imaging of the postulated action of a novel enzyme inactivator.

#### 4.2. Pharmacodynamics

PET offers an opportunity to observe key steps involved in carcinogenesis due to its ability to radiolabel and image the behaviour of several biological probes. In this section, we will describe how PET can be used to monitor various targets including genes, ligand–receptor interactions and components involved in apoptosis, drug resistance and angiogenesis.

##### 4.2.1. Evaluation of tumour metabolism and proliferation

Conventional imaging modalities for tumour response assessment relies on changes in tumour volume and mass which may not be apparent for several months after treatment and cannot easily distinguish between necrotic cells and viable, proliferating cancer cells.  $^{18}\text{F}$ -2-fluoro-2-deoxyglucose ( $^{18}\text{F}$  FDG) is being increasingly utilised as a physiological imaging modality to evaluate sub-clinical tumour response to treatment.  $^{18}\text{F}$  FDG essentially measures cellular metabolic activity, as the rate of its accumulation into tumours is proportional to the rate of glucose utilisation. Recent studies have examined changes in  $^{18}\text{F}$  FDG uptake as a pharmacodynamic endpoint after treatment of gliomas with single-agent temozolomide [63] and after combination chemotherapy in pancreatic cancer, fol-

lowing administration of 5-FU and mitomycin C [64]. Brock and colleagues [63] performed  $^{18}\text{F}$  FDG scans in patients with recurrent high-grade gliomas 7 days after treatment and found these results could predict clinical and radiological response recorded at 2 months. The European Organisation for Research and Treatment of Cancer (EORTC) PET study group have recently defined guidelines for the use of  $^{18}\text{F}$  FDG in response assessment in oncology [65].

Radiolabelled thymidine (in autoradiography and flow cytometry) has long been the gold standard for measuring DNA synthesis. PET methodology has recently been developed for measuring radiolabelled thymidine (2- $^{11}\text{C}$  thymidine) incorporation into DNA to provide an index of DNA proliferation *in vivo*. This may serve as a more direct technique of monitoring tumour response (Fig. 8) than  $^{18}\text{F}$  FDG, which is not specific for malignant tumours, and may show uptake in inflammatory cells such as macrophages. A study has shown that fractional retention of 2- $^{11}\text{C}$  thymidine-derived radioactivity correlates with MIB-1, a well established marker of cell proliferation, making 2- $^{11}\text{C}$  thymidine a suitable radiotracer for monitoring response to antiproliferative therapy. In another pilot study in patients undergoing chemotherapy, 2- $^{11}\text{C}$  thymidine flux constant measured at 1 week after treatment declined by 100% in complete responders and 35% in partial responders, compared with a much smaller decrease in a patient with progressive disease [65]. One limitation of using 2- $^{11}\text{C}$  thymidine is its

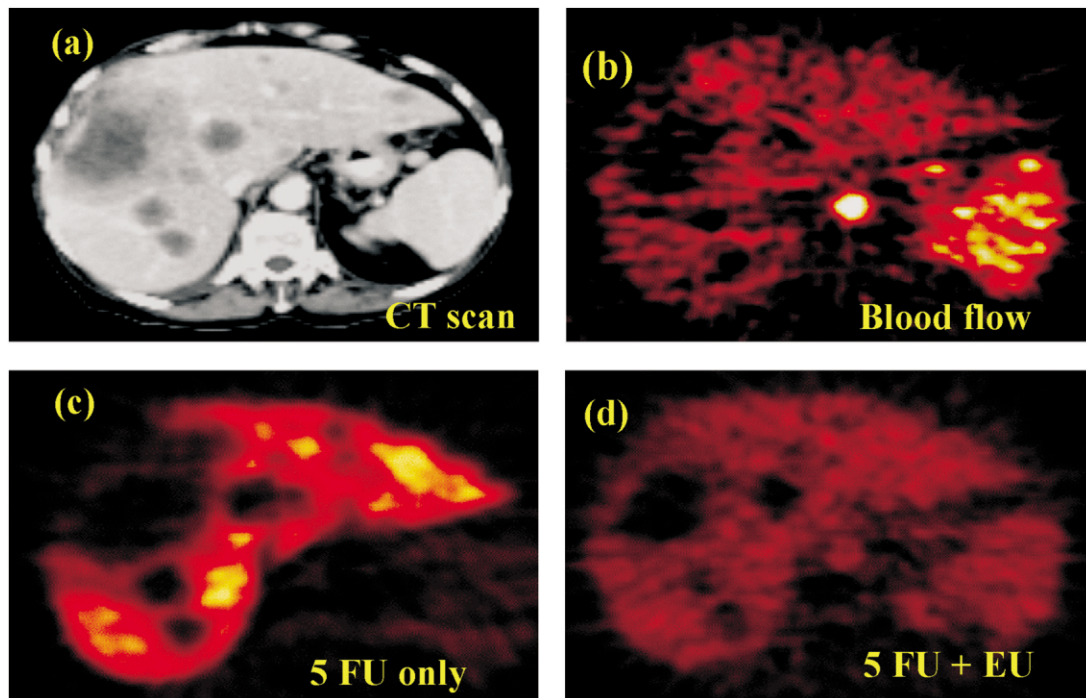


Fig. 7. Typical transabdominal Computed Tomography (CT) (a) and corresponding Positron Emission Tomography (PET) blood flow (b) and PET  $^{18}\text{F}$ -fluorouracil images without eniluracil (EU) (c) after eniluracil (d), showing liver, spleen and multiple hepatic metastasis (reprinted with permission from Elsevier Science (*Lancet* 2000 **355** 2128)).



rapid conversion to a number of systemic metabolites making data analysis difficult. An alternative, promising probe for measuring DNA proliferation is 3'-deoxy-3'-[ $^{18}\text{F}$ ] fluorothymidine (FLT) [66] which is metabolised to a lesser extent than 2-[ $^{11}\text{C}$ ] thymidine. Retention of FLT is determined not only by the degree of DNA proliferation, but also by levels of cell cycle-regulated thymidine kinase-1 protein. Detection of tumour response using PET will be advantageous in assessing new cytostatic drugs when obvious tumour shrinkage is not expected and to avoid unnecessary chemotherapy in patients not shown to have responsive disease potentially after only one course of treatment [67].

One emerging area of research is the use of 2-[ $^{11}\text{C}$ ] thymidine to measure thymidine salvage and provide an *in vivo* surrogate marker of thymidylate synthase (TS) inhibition. Increased 2-[ $^{11}\text{C}$ ]thymidine retention has been demonstrated in tumours 1 h after administration of nolatrexed, an oral TS inhibitor [68]. Another group is investigating the use of 2'-[ $^{18}\text{F}$ ]fluoro-ara-deoxyuridine to image TS activity for selection of potential patients likely to benefit from prodrugs activated by TS [69].

#### 4.2.2. Drug–receptor interaction

There are many growth factors and hormones that exert their therapeutic affect by interacting with specific receptors or binding to cell surface molecules. PET can be used to study these drug–receptor interactions with ligands or antibodies radiolabelled with a positron emitter. Such studies can either be direct (labelling the molecule of interest) or indirect (displacement of radi-

oligand by the molecule of interest). The regional kinetics of radioligands can be used to derive values for receptor number ( $B_{\text{max}}$ ), affinity ( $K_d$ ) and binding potential ( $B_{\text{max}}/K_d$ ). With the production of radioligands for hormone receptors (oestrogen [70,71], progesterone [71,72] and androgen [73–75], growth factors (vascular endothelial growth factor (VEGF) [2] and epidermal growth factor) and for C-erb2, a proto-oncogene [76], receptor studies are now being performed in oncology.

At present, the assessment of oestrogen receptor (ER) status in breast cancer relies on biopsy specimens and *in vitro* assays. This is subject to errors such as tumour heterogeneity, and provides little information regarding the responsiveness of tumour to hormonal therapy. 16 $\alpha$ -[ $^{18}\text{F}$ ] fluoro-17 $\beta$ -oestradiol (FES) has been developed as a radioligand for oestrogen receptors to assess ER status in breast tumours *in vivo*. Good overall agreement between *ex vivo* ER assays and FES-PET<sup>77</sup> has led to the conclusion that FES-PET provides direct information on ER status. A decrease in the uptake of FES in metastatic breast cancers after the administration of tamoxifen has been visualised, demonstrating the presence of functional oestrogen receptors in the tumour [78]. The reduction in FES uptake after tamoxifen was significantly greater in patients who responded to hormonal therapy [79]. PET visualised drug–receptor interaction can therefore predict response to tamoxifen therapy [80,81] and also help determine ER status where there may be doubt, for example in metastatic disease in previously ER-positive tumours [78].

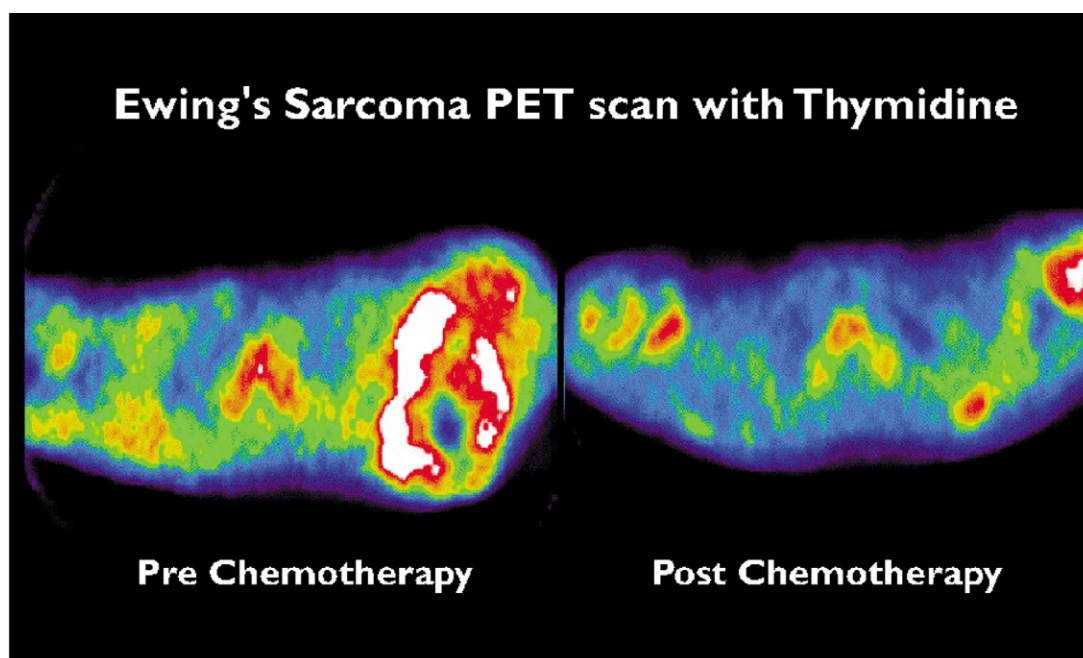


Fig. 8. 2[ $^{11}\text{C}$ ]thymidine Positron Emission Tomography (PET) scan in a patient with Ewing's sarcoma in the upper/thorax shoulder, pre- and postchemotherapy. The white area indicates the region of highest uptake. Resection revealed almost complete histological response showing the use of 2[ $^{11}\text{C}$ ]thymidine PET scan in early response assessment.

Other radioligands undergoing studies in animals are [ $^{18}\text{F}$ ]-labelled progesterin 16 alpha, 17 alpha-dioxolanes for progesterone receptors [82,83] and [ $^{18}\text{F}$ ]-labelled androgens for prostate cancer [73–75]. Recently, [ $^{64}\text{Cu}$ ]-TETA-ocretotide has shown promise as a PET radiopharmaceutical in patients with neuroendocrine tumours [84].

#### 4.2.3. Assessment and modulation of multidrug resistance

Acquired multidrug resistance (MDR) is a major obstacle to the treatment of cancer with certain classes of compounds such as anthracyclines, vinca alkaloids, podophyllotoxins and taxanes [85,86]. Several groups have identified the overexpression of P-glycoprotein (Pgp), a plasma membrane transporter encoded for by the MDR gene, as the molecular basis for the MDR phenotype [87,88]. A number of radiolabelled pharmaceuticals are being investigated to examine this process further in conjunction with strategies to block expression or activity of Pgp. Technetium-99m Sestambi ( $^{99\text{m}}\text{Tc}$ -Sestambi), a substrate for Pgp, has been used in SPECT studies to visualise blockade of Pgp-mediated transport after modulation of the Pgp pump [89]. A 2.7-fold higher efflux rate of  $^{99\text{m}}\text{Tc}$ -Sestambi has been demonstrated in breast cancers with high Pgp expression [90,91]. So far *in vivo* PET studies involved in evaluation of MDR have been confined to experimentation in animals. Carbon-11 radiolabelled drugs such as  $^{11}\text{C}$ -verapamil,  $^{11}\text{C}$ -daunorubicin [92–94] and  $^{11}\text{C}$ -colchicine [95] have been investigated as *in vivo* Pgp probes and have a potential use in the selection of patients in whom Pgp modulation may be beneficial during treatment [96].

#### 4.2.4. Quantitating angiogenesis and antivasculature activity

Angiogenesis represents a crucial step in tumour development [97] and describes neovascularisation from existing blood vessels. Many cytokines implicated in this process have been discovered including VEGF, whose levels are upregulated in several cancers such as breast, colon, ovarian and lung and which may have prognostic significance [98,99]. There are two principal therapeutic targets in angiogenesis: direct, by inhibition of angiogenic factors or receptors (anti-angiogenic agents), or indirect, by inhibition of blood flow (antivasculature agents). PET methods are being developed to measure parameters related to the angiogenic phenotype. One study has demonstrated the feasibility of imaging VEGF using an anti-VEGF antibody labelled with iodine 124- ( $^{124}\text{I}$ -VG76e) in mice bearing human xenografts. *Ex vivo* biodistribution confirmed antibody localisation within tumour [2]. PET has demonstrated the effects of the new anti-vascular agent Combrestatin A4 Phosphate (CA4P) by measuring tumour and normal tissue perfusion and blood volume [3]. In this study, PET scans with [ $^{15}\text{O}$ ]  $\text{H}_2\text{O}$  and [ $^{15}\text{O}$ ] CO were performed

on patients receiving CA4P as part of a UK Cancer Research Campaign phase 1 trial. Results showed a 30–60% temporary reduction in tumour blood flow at the higher dose level. Further analysis of data is ongoing concerning changes in blood volume. It is anticipated that these types of pharmacodynamic assessment will reduce the time involved in early clinical trials provide more objective criteria for the development of anti-angiogenic agents and recognise patients who will benefit from anti-angiogenic treatment [100].

#### 4.2.5. Detection of apoptosis

Programmed cell death is the likely mechanism behind the cytoreductive effects of standard chemotherapeutic agents. At present, there are no specific measures of this important pharmacodynamic endpoint other than *ex-vivo* analysis of tumours by immunohistochemistry or flow cytometry. Annexin V, an endogenous protein, is a new radioligand that is capable of detecting apoptosis *in vivo* due to its high (nanomolar) affinity for membrane bound phosphatidylserine [101]. An early event in apoptosis is the rapid exposure of phosphatidylserine groups, which are normally confined internally within the cell. Binding of Annexin V to these exposed phosphatidylserine groups allows apoptosed cells to be detected. Annexin V has been labelled with  $^{99\text{m}}\text{Tc}$  for imaging with single photon emitting computed tomography (SPECT) [102–104]. Annexin V has more recently been labelled with iodine 124 which can be detected with PET [119] and is being validated in preclinical studies. This will be of greater benefit in quantifying the efficacy of cytotoxic drugs.

#### 4.2.6. Tumour hypoxia

Hypoxia resulting from inadequate blood supply of oxygen to cells is an important contributor to resistance of tumours to radiotherapy and some chemotherapeutic treatments. [ $^{18}\text{F}$ ] fluoromisonidazole has been used as a PET marker to quantitate hypoxia in tumours [105–107]. Rasey and colleagues found hypoxia was present in 97% of 37 tumours when studied with [ $^{18}\text{F}$ ] fluoromisonidazole. They found a marked variation in hypoxia between tumours of the same site or histology and within regions of a single tumour. Other markers of hypoxia including SR 4554 and  $^{64}\text{Cu}$ -ATSM are being developed also for similar *in vivo* assessments of hypoxia [108,109]. Obtaining knowledge of hypoxia *in vivo* could ultimately lead to the identification of patients for treatment with drugs to enhance oxygenation or with hypoxia-targeted gene therapy.

#### 4.2.7. ADEPT

Antibody directed enzyme pro-drug therapy (ADEPT) is being explored as a way to target therapy

selectively to cancer cells. ADEPT is based on the delivery of a non-toxic antibody–enzyme conjugate specific to a tumour [110]. After a period of time, sufficient to allow for clearance of unbound conjugate, a non-toxic pro-drug is administered which is converted to a toxic compound by the conjugate. By labelling the pro-drug or conjugate with a positron emitter, it should be possible to quantitate their distribution. A pro-drug, which is a substrate for carboxypeptidase G2, has been labelled with carbon-11 for monitoring delivery and uptake using PET [111,112].

#### 4.2.8. Markers of gene expression

Advances in genetic engineering have progressed to allow therapy by transferring appropriate genes into abnormal cells. An important question related to this is accurate *in situ* monitoring and timing of gene expression, which currently can only be achieved with biopsy specimens. PET imaging can make a major contribution to this area [113,114] and several analogues of positron-emitting uracil and thymidine are being developed for this purpose [115,116]. These analogues undergo phosphorylation and trapping when Herpes Simplex Virus-1 thymidine kinase (HSV-1 tk) is expressed and this has been visualised in experimental animals [117].

## 5. Summary

Advances in technology have made *in vivo* assessment of physiological and biochemical processes in humans a reality. This has been achieved by the integrated work of a multidisciplinary team within a PET department. PET is an invaluable tool in the preclinical assessment of drugs prior to further development. Clinical assessment of drugs can help elucidate mechanisms of action, and resistance, at tracer doses. Newer therapies can be investigated where conventional methods of drug analysis will not provide the necessary information. PET methodology needs to be further developed as a translational tool to lessen the gap between drug discovery and clinical application [118].

## United references

Refs. [29,33] are not cited.

## References

- Harte RAH, Mathews JC, O'Reilly SM, *et al.* Tumour, normal tissue, and plasma pharmacokinetic studies of fluorouracil biomodulation with *N*-phosphacetyl-L-aspartate, folinic acid, and interferon alfa. *J Clin Oncol* 1999, **17**, 1580–1589.
- Carroll VA, Glaser M, Aboagye E, *et al.* Imaging vascular endothelial growth factor *in vivo* with positron emission tomography. *Br J Cancer* 2000, **83**, P6.
- Anderson H, Yap J, Price PM. Measurement of tumour and normal tissue (NT) perfusion by positron emission tomography (PET) in the evaluation of antivascular therapy: results in the phase I study of Combretastatin A4 Phosphate (CA4P). *Proc Annu Meet Am Soc Clin Oncol* 2000, **19**, 179a.
- Leonard KA, Deisseroth AB, Austin DJ. Combinatorial chemistry in cancer drug development. *Cancer J* 2001, **7**, 79–83.
- Tatum JL, Hoffman JM. Imaging drug development. *Acad Radiol* 2000, **7**, 1007–1008.
- Cambell B. Drug development and positron emission tomography. In Comar D, ed. *PET for Drug Development and Evaluation*. Dordrecht, Kluwer Academic Publishers, 1995, 1–24.
- Mintun MA, Welch MJ, Sigel CJ, Mathias JW. Breast Cancer: PET imaging of oestrogen receptors. *Radiology* 1988, **169**, 45–48.
- Brady F, Luthra SJ, Tochon-Danguy CJ. Asymmetric synthesis of S-(3'-t-butylamino-2'-hydroxypropoxy)-benzimidazol-2-[<sup>11</sup>C]one(-S-[<sup>11</sup>C]CGP 12177) as a preferred radioligand for beta-adrenergic receptors. *Int J Rad Appl Instrum* 1991, **A42**, 621–628.
- Huang SC, Phelps ME. Principles of tracer kinetic modelling in positron tomography. In Phelps ME, Mazziota JC, Schelbert HR, eds. *Positron Emission Tomography and Autoradiography: Principles and Applications for the Brain and Heart*. New York, Raven Press, 1986, 287–346.
- Gunn RN, Yap JT, Wells P, Osman S, Price PM, Jones T. A general method to correct PET data for tissue metabolites using a dual-scan approach. *J Nucl Med* 2000, **41**, 706–711.
- Blasberg RG, Roelcke U, Weinreich R, *et al.* Imaging brain tumour proliferative activity with [<sup>124</sup>I]iododeoxyuridine. *Cancer Res* 2000, **60**, 624–635.
- Saleem A, Yap J, Osman S, *et al.* Modulation of fluorouracil tissue pharmacokinetics by eniluracil: *in vivo* imaging of drug action. *Lancet* 2000, **355**, 2125–2131.
- Cunningham VJ, Jones T. Spectral analysis of dynamic PET studies. *J Cereb Blood Flow Metab* 1993, **13**, 15–23.
- Patlak CS, Blasberg RG, Fenstermacher JD. Graphical evaluation of blood-to-brain transfer constant from multiple-time uptake data. *J Cereb Blood Flow Metab* 1983, **3**, 1–7.
- Yung WK, Albright RE, Olson J, *et al.* A phase II study of temozolomide vs. procarbazine in patients with glioblastoma multiforme at first relapse. *Br J Cancer* 2000, **83**, 588–593.
- Brandes AA, Pasetto LM, Vastola F, Monfardini S. Temozolomide in patients with high grade glioma. *Oncology* 2000, **59**, 181–186.
- Prados MD. Future directions in the treatment of malignant gliomas with temozolomide. *Semin Oncol* 2000, **27**, 41–46.
- Bower M, Newlands ES, Bleehen NM, *et al.* Multicentre CRC phase II trial of temozolomide in recurrent or progressive high grade gliomas. *Cancer Chemother Pharmacol* 1997, **40**, 484–488.
- Middleton MR, Grob JJ, Aaronson N, *et al.* Randomised phase III study of temozolomide vs. dacarbazine in the treatment of patients with advanced metastatic melanoma. *J Clin Oncol* 2000, **18**, 158–166.
- Agarwala SS, Kirkwood JM. Temozolomide, a novel alkylating agent with activity in the central nervous system, may improve the treatment of advanced metastatic melanoma. *Oncologist* 2000, **5**, 144–151.
- Bleehen NM, Newlands ES, Lee S, *et al.* CRC phase II trial of temozolomide metastatic melanoma. *J Clin Oncol* 1995, **13**, 10–13.
- Estlin EJ, Lashford L, Ablett S, *et al.* Phase I study of temozolomide in paediatric patients with advanced cancer. UK Children's Cancer Study Group. *Br J Cancer* 1998, **78**, 652–661.
- Nicholson HS, Krailo M, Ames MM, *et al.* Phase I study of temozolomide in children and adolescents with recurrent solid tumours: a report from the Children's Cancer Group. *J Clin Oncol* 1998, **16**, 3037–3043.
- Woll PJ, Crowther D, Johnson PW, *et al.* Phase II trial of

- temozolomide in low-grade non-Hodgkin's lymphoma. *Br J Cancer* 1995, **72**, 183–184.
25. Van Brussel JP, Busstra MB, Lang MS, Catsburg T, Schroder FH, Mickish GH. A phase II study of temozolomide in hormone-refractory prostate cancer. *Cancer Chemother Pharmacol* 2000, **45**, 509–512.
  26. Moore MJ, Feld R, Hedley D, Oza A, Siu LL. A phase II study of temozolomide in advanced untreated pancreatic cancer. *Invest New Drugs* 1998, **16**, 77–79.
  27. Chan AT, Leung TW, Kwan WH, Mok TS, Yeo W, Lai M, Johnson PJ. Phase II study of Temodal in the treatment of patients with advanced nasopharyngeal carcinoma. *Cancer Chemother Pharmacol* 1998, **42**, 247–249.
  28. Woll PJ, Judson I, Lee SM, et al. Temozolomide in patients with advanced soft tissue sarcoma: a phase II study of the EORTC Soft Tissue and Bone Sarcoma Group. *Eur J Cancer* 1999, **35**, 410–412.
  29. Stevens MF, Newlands ES. From triazines and triazenes to temozolomide. *Eur J Cancer* 1996, **32A**, 2236–2241.
  30. Tsang LL, Quaterman CP, Gescher A, Slack JA. Comparison of the cytotoxicity of temozolomide and dacarbazine, prodrugs of 3-methyl-(triazene-1-yl)imidazole-4-carboxamide. *Cancer Chemother Pharmacol* 1991, **27**, 342–346.
  31. Brown GD, Turton DR, Luthra SK, et al. Synthesis of [<sup>11</sup>C-methyl]methylisocyanate and application of microwave heating to label the novel anticancer agent temozolomide. *J Label Radiopharm* 1994, **35**, 100–103.
  32. Meikl SR, Mathews JC, Brock CS, et al. Pharmacokinetic assessment of novel anti-cancer drugs using spectral analysis and positron emission tomography: a feasibility study. *Cancer Chemother Pharmacol* 1998, **42**, 183–193.
  33. Brock CS, Mathews JC, Brown GD, et al. The kinetic behaviour of temozolomide in man. *Proc Annu Meet Am Soc Clin Oncol* 1996, **16**, 548a.
  34. Brock CS, Mathews JC, Brown GD, et al. Temozolomide uptake in human astrocytomas demonstrated *in vivo*. *Proc Annu Meet Am Soc Clin Oncol* 1997, **16**, 231a.
  35. Brock CS, Mathews JC, Brown GD, et al. Response to temozolomide (TEM) in recurrent high grade gliomas (HGG) is related to drug concentration. *Annals Oncol* 1998, **9**, 174.
  36. Atwell GJ, Rewcastle GW, Baguley BC, Denny WA. Potential antitumour agents: 50. *In vivo* solid-tumour activity of derivatives of N-[2-(dimethylamino)ethyl]acridine-4-carboxamide. *J Med Chem* 1987, **30**, 664–669.
  37. Finlay GJ, Marshall E, Mathews JH, Paull KD, Baguley BC. *In vitro* assessment of N-[2-(dimethylamino)ethyl]acridine-4-carboxamide, a DNA-intercalating antitumour drug with reduced sensitivity to multidrug resistance. *Cancer Chemother Pharmacol* 1993, **31**, 401–406.
  38. Baguley BC, Holdaway KM, Fray LM. Design of DNA intercalators to overcome topoisomerase 2-mediated multidrug resistance. *J Natl Cancer Inst* 1990, **82**, 398–402.
  39. Baguley BC, Finlay GJ, Ching LM. Resistance mechanisms to topoisomerase poisons: the application of cell culture methods. *Oncol Res* 1992, **4**, 267–274.
  40. Baguley BC, Finlay GJ. Selectivity of N-[2-(dimethylamino)ethyl]acridine-4-carboxamide towards Lewis lung carcinoma and human tumour cell lines *in vitro*. *Eur J Cancer Clin Onc* 1989, **25**, 271–277.
  41. Brady F, Luthra SK, Brown G. Carbon-11 labelling of the antitumour agent N-[2-(dimethylamino)ethyl]acridine-4-carboxamide (DACA) and determination of plasma metabolites in man. *Appl Radiat Isot* 1997, **48**, 487–492.
  42. Brady F, Luthra SK, Turton DR. Automated radiosynthesis of [6-<sup>11</sup>C-methyl]buprornorphine from 3-O-trityl protected precursors. *Appl Radiat Isot* 1994, **45**, 857–873.
  43. Saleem A, Harte JAH, Mathews JC, et al. Pharmacokinetic evaluation of N-[2-(dimethylamino)ethyl]acridine-4-carboxamide in patients with positron emission tomography. *J Clin Oncol* 2001, **19**, 1421–1429.
  44. Twelves CJ, Gardener C, Flavin A, et al. Phase I pharmacokinetic study of DACA (XR5000): a novel inhibitor of isomerase 1 and 11. CRC Phase I/II Committee. *Br J Cancer* 1999, **80**, 1786–1791.
  45. Osman S, Luthra SK, Brady F, et al. Studies on the metabolism of the novel antitumour agent [N-methyl-<sup>11</sup>C]N-[2-(dimethylamino)ethyl]acridine-4-carboxamide in rats and humans prior to phase I clinical trials. *Cancer Res* 1997, **57**, 2172–2180.
  46. Paxton JW, Young D, Evans SM, Kestell P, Robertson IG, Cornford EM. Pharmacokinetics and toxicity of the antitumour agent N-[2-(dimethylamino)ethyl]acridine-4-carboxamide after *i.v.* administration in the mouse. *Cancer Chemother Pharmacol* 1992, **29**, 379–384.
  47. Harte JAH, Mathews JC, Flavin A, et al. Pre-phase I tracer kinetic studies in humans can contribute to new drug evaluation. *Ann Oncol* 1996, **7**, 50a.
  48. Pinedo HM, Peters GF. Fluorouracil: biochemistry and pharmacology. *J Clin Oncol* 1988, **6**, 1653–1664.
  49. Heggie GD, Sommadossi JP, Cross DS, Huster WJ, Diasio RB. Clinical pharmacokinetics of 5-fluorouracil and its metabolites in plasma, urine and bile. *Cancer Res* 1987, **47**, 2203–2206.
  50. Harte RJ, Matthews JC, O'Reilly SM, Price PM. Sources of error in tissue and tumor measurements of 5-[<sup>18</sup>F]fluorouracil. *J Nucl Med* 1998, **39**, 1370–1376.
  51. Dimitrakopoulou A, Strauss LG, Clorius JH, et al. Studies with positron emission tomography after systemic administration of fluorine-18-uracil in patients with liver metastases from colorectal carcinoma. *J Nucl Med* 1993, **34**, 1075–1081.
  52. Hohenberger P, Strauss LG, Lehner B, Frohmüller S, Dimitrakopoulou A, Schlag P. Perfusion of colorectal liver metastases and uptake of fluorouracil assessed by H<sub>2</sub>[<sup>15</sup>O] and [<sup>18</sup>F]uracil positron emission tomography (PET). *Eur J Cancer* 1993, **12**, 1682–1686.
  53. Kissel J, Brix G, Bellemann ME, Strauss LG, et al. Pharmacokinetic analysis of 5-[<sup>18</sup>F]fluorouracil tissue concentrations measured with positron emission tomography in patients with liver metastases from colorectal adenocarcinoma. *Cancer Res* 1997, **57**, 3415–3423.
  54. Moehler M, Dimitrakopoulou-Strauss A, Gutzler F, Raeth U, Strauss LG, Stremmel W. <sup>18</sup>F-labeled fluorouracil positron emission tomography and the prognoses of colorectal carcinoma patients with metastases to the liver treated with 5-fluorouracil. *Cancer* 1998, **83**, 245–253.
  55. Dimitrakopoulou-Strauss A, Strauss LG, Schlag P, et al. Intravenous and intra-arterial oxygen-15-labeled water and fluorine-18-labeled fluorouracil in patients with liver metastases from colorectal carcinoma. *J Nucl Med* 1998, **39**, 465–473.
  56. Brix G, Bellemann ME, Gerlach L, Haberkorn U. Intra- and extracellular fluorouracil uptake: assessment with contrast-enhanced metabolic F-19 MR imaging. *Radiology* 1998, **209**, 259–267.
  57. Shani J, Wolf W. A model for prediction of chemotherapy response to 5-fluorouracil based on the differential distribution of 5-[<sup>18</sup>F]fluorouracil in sensitive versus resistant lymphocytic leukemia in mice. *Cancer Res* 1977, **37**, 2306–2308.
  58. Moehler M, Dimitrakopoulou-Strauss A, Gutzler F, Raeth U, Strauss LG, Stremmel W. <sup>18</sup>F-labeled fluorouracil positron emission tomography and the prognoses of colorectal carcinoma patients with metastases to the liver treated with 5-fluorouracil. *Cancer* 1998, **83**, 245–253.
  59. Dimitrakopoulou-Strauss A, Strauss LG, Schlag P, et al. Fluorine-18-fluorouracil to predict therapy response in liver metastases from colorectal carcinoma. *J Nucl Med* 1998, **39**, 1197–1202.
  60. Presant CA, Wolf W, Albright MJ, et al. Human tumor fluorouracil trapping: clinical correlations of *in vivo* <sup>19</sup>F nuclear magnetic resonance spectroscopy pharmacokinetics. *J Clin Oncol* 1990, **8**, 1868–1873.

61. Presant CA, Wolf W, Waluch V, et al. Association of intratumoral pharmacokinetics of fluorouracil with clinical response [see comments]. *Lancet* 1994, **343**, 1184–1187.
62. Ahmed FY, Johnston SJ, Cassidy J. Eniluracil treatment completely inactivates dihydropyrimidine dehydrogenase in colorectal tumours. *J Clin Oncol* 1999, **17**, 2439–2445.
63. Brock CS, Young H, O'Reilly SM, et al. Early evaluation of tumour metabolic response using [ $^{18}\text{F}$ ]fluorodeoxyglucose and positron emission tomography: a pilot study following the phase II chemotherapy schedule for temozolomide in recurrent high-grade gliomas. *Br J Cancer* 2000, **82**, 608–615.
64. Maisey NR, Webb A, Flux GD, et al. FDG-PET in the prediction of survival of patients with cancer of the pancreas: a pilot study. *Br J Cancer* 2000, **83**, 287–293.
65. Young H, Baum R, Cremerius U, et al. Measurement of clinical and subclinical tumour response using [ $^{18}\text{F}$ ]fluorodeoxyglucose and positron emission tomography: review and 1999 EORTC recommendations. European Organization for Research and Treatment of Cancer (EORTC) PET Study Group. *Eur J Cancer* 1999, **35**, 1773–1782.
66. Shields AF, Grierson JR, Dohmen BM, et al. Imaging proliferation *in vivo* with [ $^{18}\text{F}$ ]FLT and positron emission tomography. *Nat Med* 1998, **4**, 1334–1336.
67. Price P, Jones T. Can positron emission tomography (PET) be used to detect subclinical response to cancer therapy? The EC PET Oncology Concerted Action and the EORTC PET Study Group. *Eur J Cancer* 1995, **31**, 1924–1927.
68. Wells P, Gunn RN, Hughes A, Taylor GA, Price P, Newell DR. Thymidine salvage demonstrated *in vivo* a specific pharmacodynamic endpoint of thymidylate synthase (TS) inhibition. *Am Assoc Cancer Res* 1997 (abstr), **76**, 10a.
69. Collins JM, Klecker RW, Katki AG. Suicide prodrugs activated by thymidylate synthase: rationale for treatment and non-invasive imaging of tumors with deoxyuridine analogues. *Clin Cancer Res* 1999, **5**, 1976–1981.
70. VanBrocklin HF, Liu A, Welch MJ, O'Neil JP, Katzenellenbogen JA. The synthesis of 7 alpha-methyl-substituted estrogens labeled with fluorine-18: potential breast tumor imaging agents. *Steroids* 1994, **59**, 34–45.
71. Katzenellenbogen JA, Welch MJ, Dehdashti F. The development of estrogen and progestin radiopharmaceuticals for imaging breast cancer. *Anticancer Res* 1997, **17**, 1573–1576.
72. de Groot TJ, Verhagen A, Elsinga PH, Vaalburg W. Synthesis of [ $^{18}\text{F}$ ]fluoro-labeled progestins for PET. *Int J Rad Appl Instrum [A]* 1991, **42**, 471–474.
73. Liu A, Carlson KE, Katzenellenbogen JA. Synthesis of high affinity fluorine-substituted ligands for the androgen receptor. Potential agents for imaging prostatic cancer by positron emission tomography. *J Med Chem* 1992, **35**, 2113–2129.
74. Bonasera TA, O'Neil JP, Xu M, et al. Preclinical evaluation of fluorine-18-labeled androgen receptor ligands in baboons. *J Nucl Med* 1996, **37**, 1009–1015.
75. Liu A, Dence CS, Welch MJ, Katzenellenbogen JA. Fluorine-18-labelled androgens: radiochemical synthesis and tissue distribution and studies on six fluorine-substituted androgens, potential imaging agents for prostatic cancer. *J Nucl Med* 1992, **33**, 724–734.
76. Bakir MA, Eccles S, Babich JW, et al. C-erbB2 protein overexpression in breast cancer as a target for PET using iodine-124-labeled monoclonal antibodies [published erratum appears in *J Nucl Med*, 1993 **34**, 290] [see comments]. *J Nucl Med* 1992, **33**, 2154–21560.
77. Dehdashti F, Mortimer JE, Siegel BA, et al. Positron tomographic assessment of estrogen receptors in breast cancer: comparison with FDG-PET and *in vitro* receptor assays. *J Nucl Med* 1995, **36**, 1766–1774.
78. McGuire AH, Dehdashti F, Siegel BA, et al. Positron tomographic assessment of 16 alpha-[ $^{18}\text{F}$ ] fluoro-17 beta- estradiol uptake in metastatic breast carcinoma. *J Nucl Med* 1991, **32**, 1526–1531.
79. Dehdashti F, Flanagan FL, Mortimer JE, Katzenellenbogen JA, Welch MJ, Siegel BA. Positron emission tomographic assessment of “metabolic flare” to predict response of metastatic breast cancer to antiestrogen therapy. *Eur J Nucl Med* 1999, **26**, 51–56.
80. Mortimer JE, Dehdashti F, Siegel BA, Katzenellenbogen JA, Frcasso P, Welch MJ. Positron emission tomography with 2-[ $^{18}\text{F}$ ]Fluoro-2-deoxy-D-glucose with 16 $\alpha$ -[ $^{18}\text{F}$ ] fluoro-17 $\beta$ -oestradiol in breast cancer: correlation with estrogen receptor status and response to systemic therapy. *Clin Cancer Res* 1996, **2**, 933–939.
81. Flanagan FL, Dehdashti F, Siegel BA. PET in breast cancer. *Semin Nucl Med* 1998, **28**, 290–302.
82. Buckman BO, Bonasera TA, Kirschbaum KS, Welch MJ, Katzenellenbogen JA. Fluorine-18-labelled progestin 16 alpha, 17 alpha-dioxolones: development of high-affinity ligands for the progesterone receptor with high *in vivo* site selectivity. *J Med Chem* 1995, **38**, 328–337.
83. Katzenellenbogen JA, Welch MJ, Dehdashti F. The development of estrogen and progestin radiopharmaceuticals for imaging breast cancer. *Anticancer Res* 1997, **17**, 1573–1576.
84. Anderson CJ, Dehdashti F, Cutler PD, et al. 64Cu-TETA-ocretotide as a PET imaging agent for patients with neuroendocrine tumors. *J Nucl Med* 2001, **42**, 213–221.
85. Bellamy WT, Dalton WS, Dorr RT. The clinical relevance of multi-drug resistance. *Cancer Invest* 1990, **8**, 547–562.
86. Zijlstra JG, de Vries EG, Mulder NH. Multifactorial drug resistance in an adriamycin-resistant human small cell lung carcinoma cell line. *Cancer Res* 1987, **47**, 1780–1784.
87. Gottesman MM, Pastan I. Biochemistry of multidrug resistance mediated by the multidrug transporter. *Annu Rev Biochem* 1993, **62**, 385–427.
88. Germann UA, Pastan I, Gottesman MM. P-glycoproteins: mediators of multidrug resistance. *Semin Cell Biol* 1993, **4**, 63–76.
89. Chen CC, Meadows B, Regis J, et al. Detection of *in vivo* P-glycoprotein inhibition by PSC 833 using Tc-99m sestamibi. *Clin Cancer Res* 1997, **3**, 545–552.
90. Vecchio SD, Ciarmiello A, Potena MI, et al. *In vivo* detection of multi-drug-resistant (MDR1) phenotype by technetium-99m sestamibi scan in untreated breast cancer patients [see comments]. *Eur J Nucl Med* 1997, **24**, 150–159.
91. Ciarmiello A, Del Vecchio S, Silvestro P, et al. Tumor clearance of technetium 99m-sestamibi as a predictor of response to neoadjuvant chemotherapy for locally advanced breast cancer. *J Clin Oncol* 1998, **16**, 1677–1683.
92. Hendrikse NH, de Vries EG, Eriks-Fluks L, et al. A new *in vivo* method to study P-glycoprotein transport in tumors and the blood-brain barrier. *Cancer Res* 1999a, **59**, 2411–2416.
93. Hendrikse NH, Franssen EJ, van der Graaf WT, Vaalburg W, de Vries EG. Visualization of multi-drug resistance *in vivo*. *Eur J Nucl Med* 1999, **26**, 283–293.
94. Elsinga PH, Franssen EJ, Hendrikse NH, et al. Carbon-11-labeled daunorubicin and verapamil for probing P-glycoprotein in tumors with PET. *J Nucl Med* 1996, **34**, 1571–1575.
95. Levchenko A, Mehta BM, Lee JB, et al. Evaluation of  $^{11}\text{C}$ -colchicine for PET imaging of multiple drug resistance. *J Nucl Med* 2000, **41**, 493–501.
96. Brady F, Luthra S, Brown G, et al. Radiolabelled tracers and anticancer drugs for assessment of therapeutic efficacy using PET. *Curr Pharm Des* 2001, **7**, 1863–1892.
97. Folkman J. Tumor angiogenesis: therapeutic implications. *N Engl J Med* 1971, **285**, 1182–1186.
98. Poon RT, Fan ST, Wong J. Clinical applications of circulating angiogenic factors in cancer patients. *J Clin Onc* 2001, **19**, 1207–1225.



99. Miller KD, Sweeney CJ, Sledge GW. Redefining the target: chemotherapeutics as antiangiogenesis. *J Clin Onc* 2001, **19**, 1195–1206.
100. Weber WA, Haubner R, Vabulien E, Kuhnast B, Webster HJ, Schwaiger M. Tumour angiogenesis targeting using imaging agents. *Q J Nucl Med* 2001, **45**, 179–182.
101. Blankenberg FG, Katsikis PD, Tait JF, et al. *In vivo* detection and imaging of phosphatidylserine expression during programmed cell death. *Proc Natl Acad Sci* 1998, **95**, 6349–6354.
102. Blankenberg FG, Trauss HW. Will imaging of apoptosis play a role in clinical care? A tale of mice and men. *Apoptosis* 2001, **61**, 117–1123.
103. Blankenberg FG, Katsikis PD, Tait JF, et al. Imaging of apoptosis (programmed cell death) with <sup>99m</sup>Tc annexin V. *J Nucl Med* 1999, **40**, 184–191.
104. Yang DJ, Azhdarinia A, Wu P, et al. *In vivo* and *in vitro* measurement of apoptosis in breast cancer cells using <sup>99m</sup>Tc-Ec-annexin V. *Cancer Biotherapy and Radiopharmaceuticals* 2001, **16**, 73–78.
105. Casciari JJ, Graham MM, Rasey JS. A modeling approach for quantifying tumor hypoxia with [F-18]fluoromisonidazole PET time-activity data. *Med Phys* 1995, **22**, 1127–1139.
106. Koh WJ, Bergman KS, Rasey JS, et al. Evaluation of oxygenation status during fractionated radiotherapy in human nonsmall cell lung cancers using [F-18]fluoromisonidazole positron emission tomography. *Int J Radiat Oncol Biol Phys* 1995, **33**, 391–398.
107. Rasey JS, Koh WJ, Evans ML, et al. Quantifying regional hypoxia in human tumors with positron emission tomography of [<sup>18</sup>F]fluoromisonidazole: a pretherapy study of 37 patients. *Int J Radiat Oncol Biol Phys* 1996, **36**, 417–428.
108. Aboagye EO, Kelson AB, Tracy M, Workman P. Preclinical development and current status of the fluorinated 2-nitroimidazole hypoxia probe N-(2-hydroxy-3,3,3-trifluoropropyl)-2-(2-nitro-1-imidazolyl) acetamide (SR 4554, CRC 94/17): a non-invasive diagnostic probe for the measurement of tumor hypoxia by magnetic resonance spectroscopy and imaging, and by positron emission tomography. *Anticancer Drug Des* 1998, **13**, 703–730.
109. Lewis JS, McCarthy DW, McCarthy TJ, Fujibayashi Y, Welch MJ. Evaluation of <sup>64</sup>Cu-ATSM *in vitro* and *in vivo* in a hypoxic tumour model. *J Nucl Med* 1999, **40**, 177–183.
110. Blakey DC, Burke PJ, Davies DH, et al. Antibody-directed enzyme prodrug therapy (ADEPT) for treatment of major solid tumour disease. *Biochem Soc Trans* 1995, **23**, 1047–1050.
111. Prenant C, Shah F, Brady F, et al. Synthesis of [<sup>11</sup>C]chloroethyl-triflate from [<sup>11</sup>C] ethylene; a reagent for introducing the haloethyl group into antibody directed enzyme prodrugs (ADEPT). *J Label Compds Radiopharm* 1995, **37**, 95–97.
112. Prenant C, Brady F, Luthra SK, Brown D, Burke PJ, Price P. An alternative synthesis of [<sup>11</sup>C]ethylene and conversion to [<sup>11</sup>C]chloroethyltosylate *in situ* via [<sup>11</sup>C]1-chloro-2-iodoethane for radiolabelling ADEPT prodrugs. *J Label Compd Radiopharm* 1997, **40**, 766–767.
113. Weissleder R. Molecular imaging: exploring the next frontier [editorial]. *Radiology* 1999, **212**, 609–614.
114. Wunderbaldinger P, Bogdanov A, Weissleder R. New approaches for imaging in gene therapy. *Eur J Radiol* 2000, **34**, 156–165.
115. Tjuvajev JG, Avril N, Oku T, et al. Imaging herpes virus thymidine kinase gene transfer and expression by positron emission tomography. *Cancer Res* 1998, **58**, 4333–4341.
116. Gambhir SS, Barrio JR, Phelps ME, et al. Imaging adenoviral-directed reporter gene expression in living animals with positron emission tomography. *Proc Natl Acad Sci* 1999, **96**, 2333–2338.
117. Blakey DC, Burke PJ, Davies DH, et al. Antibody-directed enzyme prodrug therapy (ADEPT) for treatment of major solid tumour disease. *Biochem Soc Trans* 1995, **23**, 1047–1050.
118. Saleem A, Aboagye E, Price PM. *In vivo* monitoring of drugs using radiotracer techniques. *Adv Drug Deliv Rev* 2000, **41**, 21–39.
119. Glaser M, Collingridge D, et al. Preparation of (124-I)IBA-Annexin-V as a potential Probe for Apoptosis. Interlaken, Switzerland, ISCR 2001 (abstr).
120. Saleem A, Osman S, Brown G, et al. Evaluation of *in vivo* mechanism of action of temozolomide. In *Proc. Annu. Meet. Am. Soc. Clin. Oncol., General Poster* 452, 2001.